JGR Solid Earth

RESEARCH ARTICLE
10.1029/2018JB016480

Active Convergence of the India-Burma-Sunda Plates Revealed by a New Continuous GPS Network

Rishav Mallick[1,2], **Eric O. Lindsey**[1], **Lujia Feng**[1], **Judith Hubbard**[1,2], **Paramesh Banerjee**[1], **and Emma M. Hill**[1,2]

[1]Earth Observatory of Singapore, Nanyang Technological University, Singapore, [2]Asian School of the Environment, Nanyang Technological University, Singapore

Key Points:
- We demonstrate active convergence between India and Burma using 2-D and 3-D plate motion models
- The Rakhine-Bangladesh megathrust is the most likely candidate to accommodate ~18 mm/year of India-Burma convergence
- Strain partitioning is necessary within the Indo-Burman Wedge, and we can place an upper bound of 8 mm/year on the slip rate of the Churachandpur-Mao Fault

Supporting Information:
- Supporting Information S1
- Data Set S1

Correspondence to:
R. Mallick,
rishav001@e.ntu.edu.sg

Citation:
Mallick, R., Lindsey, E. O., Feng, L., Hubbard, J., Banerjee, P., & Hill, E. M. (2019). Active convergence of the India-Burma-Sunda plates revealed by a new continuous GPS network. *Journal of Geophysical Research: Solid Earth*, *124*, 3155–3171. https://doi.org/10.1029/2018JB016480

Received 31 JUL 2018
Accepted 23 FEB 2019
Accepted article online 27 FEB 2019
Published online 25 MAR 2019

©2019. The Authors.
This is an open access article under the terms of the Creative Commons Attribution-NonCommercial-NoDerivs License, which permits use and distribution in any medium, provided the original work is properly cited, the use is non-commercial and no modifications or adaptations are made.

Abstract The Rakhine (Arakan)-Bangladesh megathrust, along which the Indian and Burma plates collide, is assumed by some to be inactive/aseismic due to the lack of notable interplate earthquakes in the modern instrumental catalog. However, geological and historical evidence of the great 1762 Arakan earthquake suggest the megathrust can produce *M*~8 events that could adversely affect the lives of millions of people in the region. To investigate the seismogenic potential and determine the slip budget of the megathrust, we first need to solve for India-Burma-Sunda relative plate motions. We present a new set of 24 GPS velocities (2011–2017) from the Myanmar-India-Bangladesh-Bhutan continuous GPS network. We use the new velocities and those from previously published studies to explore the geometries and slip rates of three major faults (Rakhine-Bangladesh megathrust, Churachandpur-Mao Fault, and Sagaing Fault) that accommodate the India-Burma-Sunda plate motion. Our results suggest that the three major faults we studied are likely fully coupled; the modern shortening rate across the Burma plate is 12–24 mm/year, while the total dextral shear rate is 25–32 mm/year. The possibly fully coupled shallow megathrust, and splay faults that may sole into it, are geodetically invisible while they are not slipping. However, we can identify the transition from coupling to steady creep on the deeper extension of the megathrust; we use this to show active oblique India-Burma convergence and to map along-strike and along-dip variations in dip-slip and strike-slip motion. This implies that the megathrust is currently accumulating strain which will eventually be released in earthquakes.

1. Introduction

The Rakhine-Bangladesh megathrust (variously known as the northern Sunda megathrust south of 18°N, the Rakhine (or Arakan) megathrust from 18–22°N, and the Bangladesh megathrust from 22–25°N) is the plate boundary between the Indian and Burma plates (Figure 1). The megathrust, which accommodates the subduction of the Indian plate beneath the Burma plate, has resulted from the oblique collision between the Indian and Sunda plates since the Eocene (Meng et al., 2012). The obliquity in India-Burma motion is accommodated by some combination of the megathrust, Churachandpur-Mao Fault (CMF), and other unmapped structures within the Indo-Burman Wedge (IBW). To the east of this oblique convergent margin, the ~1,200-km-long right-lateral strike-slip Sagaing Fault forms the eastern boundary of the Burma plate and accommodates the remainder of the relative plate motion between the Indian and Sunda plates (Gahalaut et al., 2013; Maurin et al., 2010; Socquet et al., 2006; Steckler et al., 2016; Vigny et al., 2003). This system of faults terminates northward into the Shillong Plateau and the Eastern Himalayan Syntaxis.

From south to north along the megathrust (18–25°N), there is a dramatic increase in the cumulative sediment input from the Ganga and Brahmaputra river systems into the Bengal Basin, the thickness of which varies from 8 to 20 km (Radhakrishna et al., 2010). The collision of these sediments with the Burma plate has subaerially exposed subduction/accretion structures within the overriding plate, such as the outer and inner IBW. The outer IBW is composed of Neogene clastic sequences affected by a series of asymmetric folds (Maurin & Rangin, 2009); this is well expressed in Bangladesh as the Chittagong-Tripura Fold Belt (Figure 1). The inner IBW rises as the Indo-Burman Ranges (IBR), further divided into the western IBR, consisting of Cretaceous flysch overlain by Paleogene sandstone, and eastern IBR, comprising Triassic flysch and Jurassic ophiolites (Sloan et al., 2017).

The western IBR hosts the CMF, which is likely an over-steepened Neogene thrust (Uddin & Lundberg, 1998), currently thought to be reactivated as a dextral strike-slip fault (Gahalaut et al., 2013; Wang et al.,

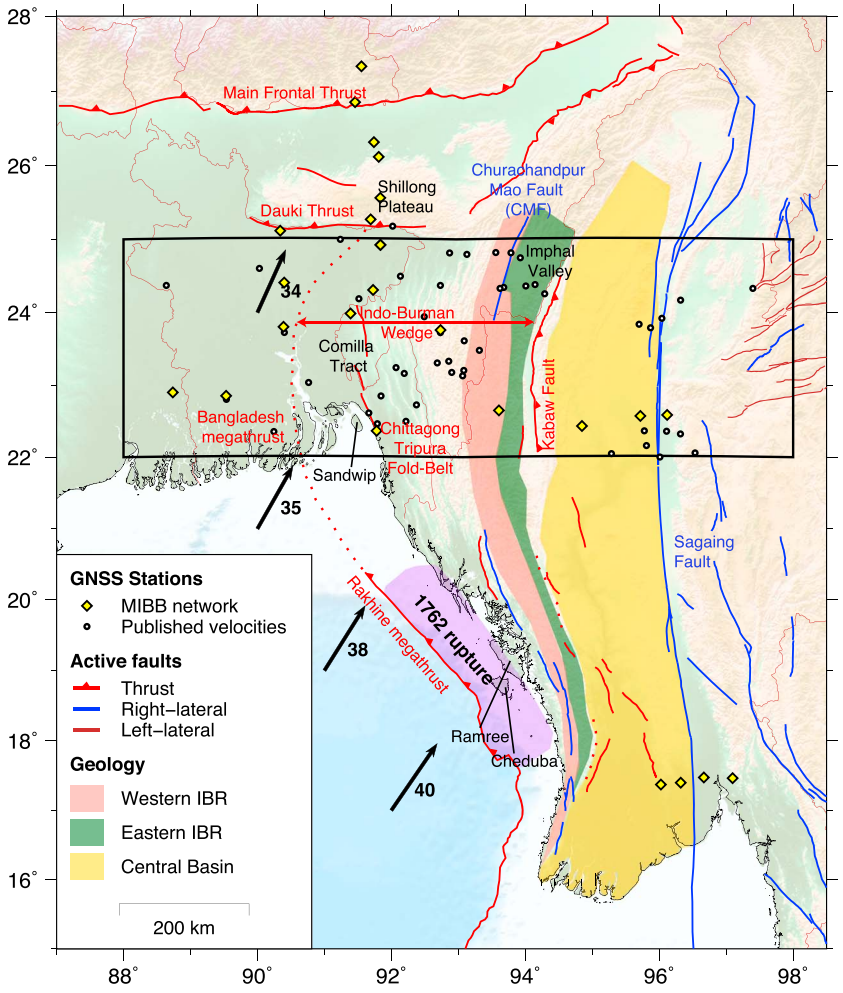

Figure 1. Overview of the study area discussed in this paper. MIBB continuous GPS stations are shown as yellow diamonds, while other published GPS velocities (Gahalaut et al., 2013; Kreemer et al., 2014; Steckler et al., 2016) are shown as white circles. The IBR are divided into the western IBR and eastern IBR based on their geology. The rupture area of the 1762 *M*~8 Great Arakan earthquake is marked in purple. The black arrows show the direction and magnitude (mm/year) of motion of India with respect to the Shan block from our model. IBR = Indo-Burman ranges; MIBB = Myanmar-India-Bangladesh-Bhutan.

2014). The CMF is clearly mapped at the surface near the Imphal Valley (Figure 1), south of which it either terminates or becomes obscured. This fault is hypothesized to accommodate a significant amount of dextral shear (~18 mm/year) resulting from the India-Burma plate motion (Gahalaut et al., 2013; Wang et al., 2014).

On the eastern edge of the eastern IBR, the east dipping Kabaw Fault separates two blocks of contrasting material, the Triassic flysch and Jurassic ophiolites of the eastern IBR and the Cretaceous sandstones overlain by young fluvial sediments of the Myanmar Central Basin (MCB; Nielsen et al., 2004; Sloan et al., 2017). The contribution of the Kabaw Fault to the strain budget of the India-Burma-Sunda system is uncertain due to an absence of clear geomorphic indicators of recent activity (Wang et al., 2014).

The eastern edge of the MCB is marked by the Sagaing Fault, a dextral strike-slip fault accommodating ~18–20 mm/year of the Burma-Sunda motion in an almost purely north-south direction (Bertrand et al., 1998; Maurin et al., 2010; Vigny et al., 2003; Wang et al., 2014).

The description of the tectonic setting highlights that the deformation associated with the eastern boundary of the Burma plate, the Sagaing Fault, is well constrained from neotectonic studies (Bertrand et al., 1998) as

well as modern geodetic investigations (Maurin et al., 2010; Vigny et al., 2003). However, modern contributions of active structures within the MCB and the IBW to the India-Burma-Sunda plate motion are poorly understood. This makes it difficult to assess the current deformational field and has led to controversies and contrasting opinions about major structures in this tectonic area. Here we focus on the question of ongoing convergence between the Indian and Burma plates and the total slip budget available to faults in the IBW.

1.1. Convergence of India and Burma Plates

The presence of a subducted Indian slab imaged beneath the Burma plate implies that subduction of the Indian slab occurred sometime in the past and drove the convergence between the India and Burma plates (Bijwaard et al., 1998; Pesicek et al., 2010; Raoof et al., 2017). However, the absence of notable seismicity on the interface between the India and Burma plates has led some authors to speculate that subduction of the Indian slab has ceased or continues purely aseismically (le Dain et al., 1984; Ni et al., 1989). The north-south directed compressive axes of well-located earthquakes ($M_w > 4$) within the downgoing Indian slab have been used to suggest that the greatest stressing rate is due to collision of India and Eurasia, not the subduction of India beneath Burma (Gahalaut et al., 2013; Le Dain et al., 1984; Ni et al., 1989). Deep intraslab earthquakes (>90 km) display tensional axes aligned with slab dip, and based on this some authors (Rangin et al., 2013; Rao & Kalpna, 2005) propose that the slab is beginning to break off and subduction has ceased and the convergence, if any, must be driven by upper plate processes.

The geology records the history of the upper plate. Youthful deformation of anticlines on Sandwip Island, and possibly the Comilla Tract (Figure 1) and uplifted marine terraces on the islands of Cheduba and Ramree (Figure 1), indicates continued inelastic deformation of continental shelf sediments in the Holocene (Aung et al., 2008; Brunnschweiler, 1966). These observations indicate that the active deformation front of the megathrust extends at least to the mouth of the Ganga-Brahmaputra delta in Bangladesh, presumably accommodated by the mapped fold and thrust belt (Betka et al., 2018; Maurin & Rangin, 2009; Nielsen et al., 2004; Steckler et al., 2008). Further south, in Myanmar, the Rakhine megathrust seems to slip on average every 500–1000 years and may have slipped all the way to the trench in the great 1762 Arakan earthquake (Wang et al., 2013).

In summary, the seismological observations have been interpreted to imply ceased or aseismic subduction, while the geological evidence suggests there is continued convergence between the India and Burma plates that results in earthquakes.

1.2. Plate Kinematics From Geodetic Studies

Past geodetic studies of the India-Burma collision zone are antithetical about the convergence across the Rakhine-Bangladesh megathrust. These studies typically use computationally inexpensive, two-dimensional dislocation models, neglecting along-strike variations in relative plate motion. Gahalaut et al. (2013) modeled campaign and continuous GPS in India and Myanmar using a two-dimensional elastic dislocation model. They infer a strike-slip rate of 18 mm/year between the India and Burma plates accommodated on the CMF, with the shallow interface creeping interseismically at ~8 mm/year. They note that there is no significant fault-perpendicular motion across their 200-km-wide profile, implying no active convergence across the northern IBW. In this model, the India-Burma plate boundary is a strike-slip fault located within the IBW, with the rest of India-Sunda motion localized on the Sagaing Fault. More recently, Steckler et al. (2016) used two-dimensional models of horizontal GPS velocities from a wider area (comprising Bangladesh, India, and Myanmar) to identify active convergence and elastic strain accumulation between the India and Burma plates. They infer a convergence rate of 13–17 mm/year between the India and Burma plates within the central IBW, with the Rakhine-Bangladesh megathrust the most likely candidate for the fault accommodating this strain budget. Steckler et al. (2016) do not explicitly invert for the strike-slip component of relative plate motion but rather impose published slip rates for the Sagaing Fault and CMF to fit the data. They further hypothesize that oblique motion on the Kabaw Fault could accommodate up to 6 mm/year of the India-Sunda plate motion.

This discrepancy in estimated convergence across the megathrust is primarily due to differences in data coverage. The addition of data from Bangladesh allows Steckler et al. (2016) to fit an elastic dislocation

model to a data transect that is 1,000 km wide and that shows an increase in the fold-belt-perpendicular velocities from Bangladesh to Myanmar (supporting information Figure S2). However, both models impose relative plate motion as a simple translation, neglecting the fact that on a spherical earth there are no rigid-body translations; there are only rigid rotations. A possible way to tackle this problem is to use block modeling, which correctly accounts for spatially variable plate velocities by considering plate motions on a sphere (McCaffrey, 2002; Meade & Loveless, 2009). Block modeling of the India-Sunda motion with GPS data has been attempted in the past with sparse data sets (Socquet et al., 2006) and was used to infer 36–39 mm/year of total relative India-Sunda motion between 18°N and 24°N. The Sagaing Fault takes up 18 mm/year of this motion as dextral strike slip, while the rest is accommodated on the Rakhine-Bangladesh megathrust and/or faults in the IBW. Socquet et al. (2006) used mostly campaign stations in Myanmar and provided only a preliminary view of the India-Burma-Sunda system. We can now refine and update those results.

In this paper, we complement previously published GPS data with the new continuous Myanmar-India-Bangladesh-Bhutan (MIBB) GPS network and use these data to model the deformation field in this complex tectonic region. We model the convergence and dextral shear rates across the region using block rotations and elastic dislocation models and use our results to answer the following fundamental questions:

1. Is there geodetically observable convergence across the Rakhine megathrust and its northern extension, the Bangladesh megathrust?
2. How is strain partitioned between the megathrust and upper-plate structures?

2. GPS Data and Analysis

2.1. MIBB GPS Data

The MIBB GPS network is a continuously operating regional network that was established in 2011. In this paper, we report the time series and velocities of 24 stations in the network (2011–2017; Figures 2 and 3). These are distributed as east-west and north-south transects crossing the Bangladesh megathrust, CMF, Sagaing Fault, Dauki Thrust, and the Main Frontal Thrust of the eastern Himalayas (yellow vectors in Figure 2).

2.2. GPS Data Processing

We process data for all 24 stations for the period of 2011–2017 using the GPS-Inferred Positioning System and Orbit Analysis Simulation Software version 6.2 and NASA Jet Propulsion Lab final precise satellite orbits and clocks. We solve for the daily positions in the International Terrestrial Reference Frame 2008 (ITRF2008; Altamimi et al., 2012; Figure 3). We use the procedure described in Feng et al. (2015) to calculate interseismic velocities. In short, we model the time series at each station as a combination of two main signals: (1) a steady interseismic velocity, which we assume is the linear rate at which plate motion is accommodated between earthquakes, (2) seasonal oscillations, modeled as annual and semi-annual sinusoids. For the stations SDWN and SWBO, which showed significant coseismic and postseismic signals from the M_w 6.8 Thabeikkyin earthquake in 2012, we added signals related to earthquake deformation (i.e., heaviside functions for coseismic offsets and logarithmic decays for postseismic processes). We used a least squares estimator to calculate the interseismic velocity at each station (Feng et al., 2015). To calculate the uncertainties in the velocities, we compute the inverse of the Jacobian, which is a matrix of partial derivatives of the data with respect to all the model parameters, and scale it using the temporal correlation of the residuals with the First Order Gauss-Markov EXponential algorithm (Herring, 2003). We present the station velocities and uncertainties in Table S1; the residuals from the fits are shown in Figure S9.

2.3. Station Velocities

We model interseismic velocities as the superposition of the velocity field from rigid block rotations and elastic strain accumulation on kinematically coupled plate interfaces. We exclude stations affected by coseismic and postseismic processes (SDWN and SWBO) since we are not investigating the effects of the earthquake cycle in this study. We combined the velocities from our data set with other published velocities for the region using the solutions obtained by Gahalaut et al. (2013), Kreemer et al. (2014) and Steckler et al.

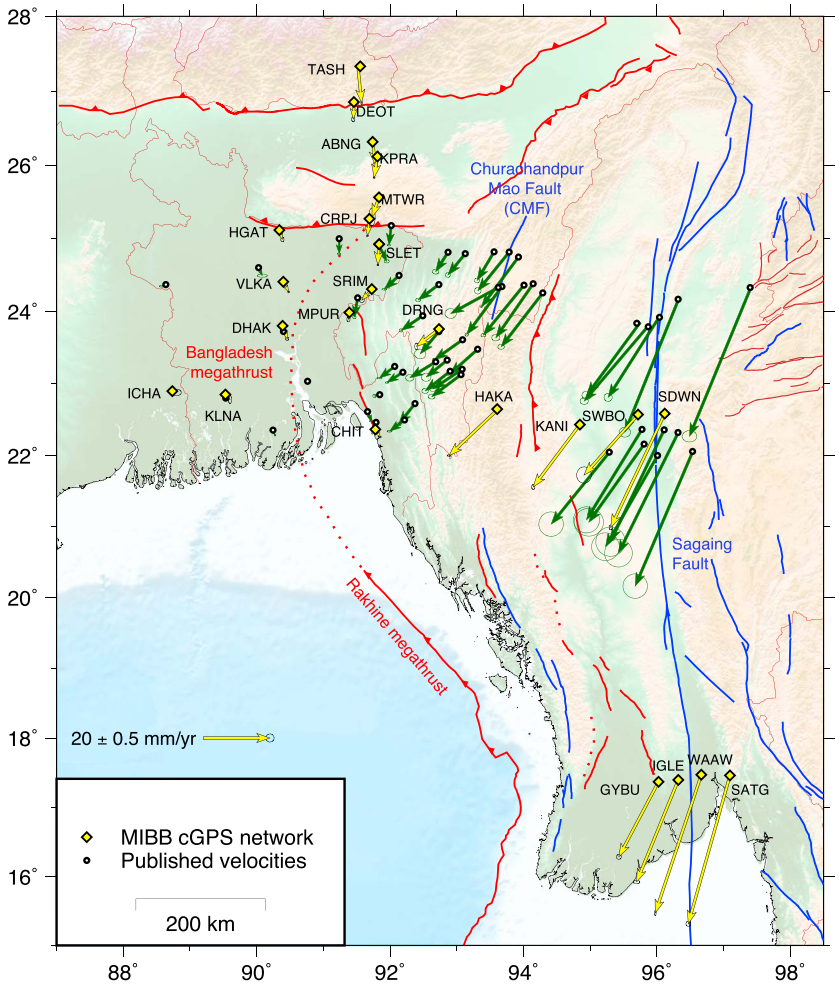

Figure 2. Map of MIBB station velocities in the India reference frame presented in this paper are shown in yellow. The labels refer to their four-character unique station ID. We combined these velocities with published velocities (Gahalaut et al., 2013; Kreemer et al., 2014; Steckler et al., 2016), shown in dark green. The uncertainty ellipses show the 95% confidence interval of the mean velocities associated with each station. MIBB = Myanmar-India-Bangladesh-Bhutan; GPS = Global Positioning System.

(2016) in ITRF2008 (Table S1). We rotate all the velocities into the Indian reference frame using the India-ITRF2008 Euler pole (latitude = 51.42°, longitude = 2.10°, rotation rate = 0.5146 x 10^{-6} °/year) presented in Steckler et al. (2016). We limit our analysis to strain accumulation in the Burma plate between 22°N and 25°N, which is where we have good station coverage. We do not use the vertical velocity components, since local site effects and extreme seasonal variations in atmospheric and hydrological loading likely contribute a larger signal than tectonics (Figure 3).

3. Inversion and Results

We parameterize our preferred model through an objective optimization of model parameters and prior constraints using Akaike's Bayesian information criterion (ABIC) following Funning et al. (2014). Our model parameters $\boldsymbol{m}^*$ are block translation rates and fault geometry parameters (for the 2-D problem); for the 3-D block modeling problem our model parameters are the angular velocity vectors for each block, the horizontal strain rate tensor for internally deforming blocks, and the weight of the dip-slip penalty hyperparameter $\sigma^2_{\text{slip rate}}$ (defined later in section 3.2, and Text S4).

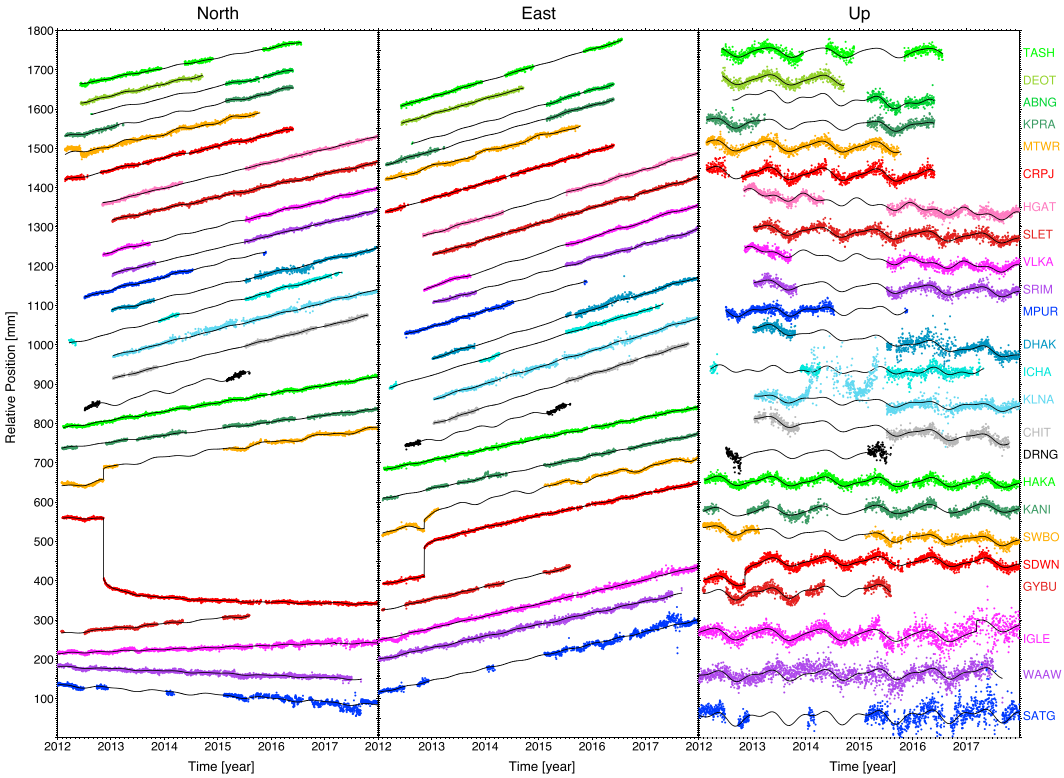

Figure 3. Three-component position time series for 24 Myanmar-India-Bangladesh-Bhutan stations in ITRF2008 (Altamimi et al., 2011). Each of the components of the time series have been assigned an arbitrary constant shift to aide in visualization. The black lines show the fit to the time series at every station using the method described in Feng et al. (2015). The stations are arranged from top to bottom: two stations in Bhutan, seven stations in Bangladesh, seven stations in India, and eight stations in Myanmar.

For a given data set $\boldsymbol{d}=\begin{bmatrix}\boldsymbol{d}_{\mathbf{GPS}}\\ \boldsymbol{d}_{\mathbf{slip\ rate}}\end{bmatrix}$ consisting of observed GPS velocities, and a priori known slip rates, with data uncertainties embedded in the covariance matrix $C_d=\begin{bmatrix}C_{d_{\mathrm{GPS}}} & 0\\ 0 & \sigma^2_{\mathrm{slip\ rate}}C_{d_{\mathrm{slip\ rate}}}\end{bmatrix}$ and a linear model $G=\begin{bmatrix}G_{\mathrm{GPS}}\\ G_{\mathrm{slip\ rate}}\end{bmatrix}$, we define *ABIC* as follows:

$$ABIC\left(\sigma^2_{\mathrm{slip\ rate}}\right)=N\log S(\boldsymbol{m}^*)+\log|G^TW\left(\sigma^2_{\mathrm{slip\ rate}}\right)G|+\log\left|W^{-1}\left(\sigma^2_{\mathrm{slip\ rate}}\right)\right|+\kappa$$

We define the weighting function W as C_d^{-1}. κ is independent of $\sigma^2_{\mathrm{slip\ rate}}$ but depends on the number of model parameters and hyperparameters.

Here $S(\boldsymbol{m}^*)=(\boldsymbol{d}-G\boldsymbol{m}^*)^TW\left(\sigma^2_{\mathrm{slip\ rate}}\right)(\boldsymbol{d}-G\boldsymbol{m}^*)$ and $\boldsymbol{m}^*=\left(G^TW\left(\sigma^2_{\mathrm{slip\ rate}}\right)G\right)^{-1}G^TW\left(\sigma^2_{\mathrm{slip\ rate}}\right)\boldsymbol{d}$ is the least squares solution to the linear inverse problem (Menke, 2012). We define $N=N_{\mathrm{GPS}}+N_{\mathrm{slip\ rate}}-M$ where N_{GPS} is the total number of GPS observations, $N_{\mathrm{slip\ rate}}$ is the total number of slip rate constraint equations, and M is the total number of model parameters. The operator $|A|$ on a square matrix A is defined as the product of the absolute values of its nonzero eigenvalues.

We also test for the significance of error improvement between different models A and B using the F test (Menke, 2012). The test statistic is defined as $F_{AB}=\frac{\chi^2_A/DF_A}{\chi^2_B/DF_B}$, and we test the probability $p\left(F<\frac{1}{F_{AB}}\ or\ F>F_{AB}\right)$ of the improvement in error having occurred by random chance using the asymmetric F distribution (Menke, 2012). Here $DF=\mathrm{N}$ refers to the degrees of freedom in the model.

3.1. Constructing Fault Geometry

We assume that the shallow part of each fault is fully coupled (not slipping) while the deeper extension, below the brittle-ductile transition, is creeping steadily at the plate rate; this coupled-uncoupled transition, henceforth referred to as the coupling transition, has a significant geodetic signal associated with it which we can fit with an elastic model (Figures S1–S2). Our model has three major faults (the Rakhine-Bangladesh megathrust, CMF, and the Sagaing Fault), and therefore three coupling transitions. We find the best fitting model geometry by first using two-dimensional semi-infinite dislocations (representing the creeping side of the transition) to investigate the locations of these coupling transitions and the magnitude of strain accumulation (Mansinha et al., 1971; Segall, 2010). We use a Markov chain Monte Carlo method to sample a suite of possible models that can fit the GPS data set (for a detailed description of the method see Text S1; Lindsey & Fialko, 2013; Neal, 2003).

We find that the horizontal locations of the deep coupling transitions for the megathrust and CMF are merely ~50 km away from each other (Figure S2), located below the inner IBW. Our constraints on depth are poor (Figures S5 and S6 and Text S2.1), but our models suggest that the depths of the coupling transitions must be greater than 25 km, with a best fitting value of ~30 km for both faults (Text S2.1; Syracuse et al., 2010). The slip rate and deep coupling transition location of the Sagaing Fault are much better constrained (Figure S6); it is consistently ~5 km east of its surface trace, implying that the fault dips ~70° toward the east. Using the location of the inferred coupling transition for the down-dip extent of the faults, and the mapped traces (CMF and Sagaing Fault) or the inferred trace of the deformation front (Rakhine-Bangladesh megathrust) for the up-dip extent of the fault, we create arcuate fault geometries for the shallow portion of the three faults (Figure 4). This step is necessary because block modeling treats elastic dislocations in the back-slip sense while our 2-D models used deep dislocations. However, both methods are most sensitive to the horizontal location of the coupling transition, which creates the strongest surface velocity gradients. We use this three-dimensional geometry to set up a block model on a spherical earth using the Blocks software (Meade & Loveless, 2009).

3.2. Block Modeling

The total width of the study area is ~1,000 km. At this scale, the curvature of the Earth and resulting plate rotations play a significant role in the observed surface velocity field. The interseismic velocities for stations far from plate boundaries vary due to rigid body rotations about an Euler pole. Deviations from these block-like motions arise due to strain accumulation on faults (block boundaries), or to internal strain within the block itself (McCaffrey, 2002). We use the software Blocks to carry out our modeling (Meade & Loveless, 2009).

We choose the Indian Block as our "reference block" with respect to which we define the velocity field. We include interseismic velocities from the IGS reference stations HYDE, IISC, and BAN2 to define the stable Indian Block. We create a model with four blocks: the Indian Block (INDIA), IBW, MCB, and Shan Block (SHAN). A point to note here is that our GPS stations do not directly sample the Sunda plate, and so we use the Shan block as a proxy for the Sunda plate.

These blocks are bounded by the megathrust, the CMF, and the Sagaing Fault (Figures 4 and 5). These faults accumulate strain and cause distortions in the surface velocity field that we model using the back-slip formulation (Okada, 1986; Savage, 1983). We allow a uniform internal strain rate field in some of our models as it acts as a proxy to describe deviations from the ideal "elastic" description of a block, instead of breaking up the IBW into further smaller blocks (e.g., Bradley et al., 2017; Thatcher, 2007). This deviation might be due to slip on multiple faults within the IBW or to diffuse deformation of the wedge material within the IBW; we cannot distinguish between these options given our current station density.

We compute the best fitting Euler poles from Blocks using the geometry we inferred from the 2-D models. We then fix the geometry of the CMF and Sagaing Fault and use the grid search algorithm to determine the best fitting coupling transition depth and fault dip for the Rakhine-Bangladesh megathrust (Figures 6a and 6b), which are nonlinear parameters, and compare it to the 2-D case. We explore a suite of models with varying levels of dip-slip penalization on the CMF, for cases of a rigid IBW as well as an internally deforming IBW and test the statistical significance of these models.

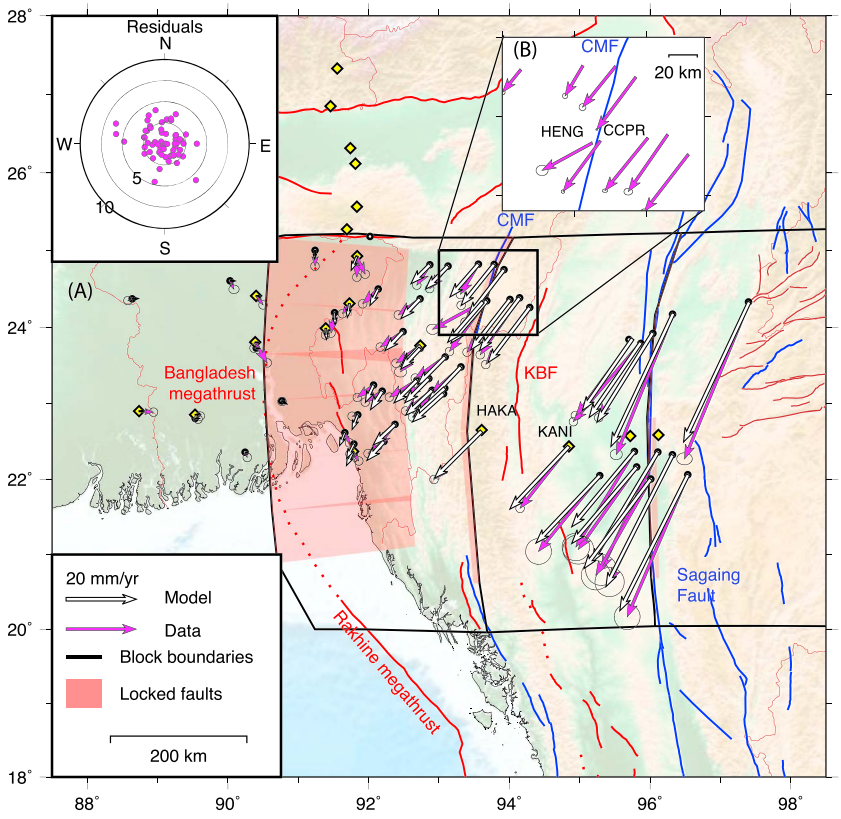

Figure 4. (a) Comparison of data and model fits from our preferred block model (rigid blocks; dip-slip prior of 0 ± 4 mm/year on the CMF; strike-slip prior of 20 ± 2 mm/year on the Sagaing fault). We find that a fully coupled fault model can explain the data reasonably well. This confirms our null hypothesis that the residual distribution (see inset figure) is a standard normal distribution; this implies that our model is a statistically feasible representation of reality. HAKA and KANI are marked in this figure to show that we do not need to invoke slip on the KBF to fit the velocities. (b) Zoom into the CMF. The stations HENG and CCPR are ~4 km apart but show dissimilar velocities, while sites to the north show a continuously varying velocity field indicating local site effects, not plate boundary creep. CMF = Churachandpur-Mao Fault; KBF = Kabaw fault.

3.3. Results

Our block modeling results are shown in Figures 4–7 and S10. All models show convergence between the Indian Block and the IBW, with at least 12 mm/year of shortening/arc-perpendicular motion between the blocks (Figures 5 and S6–S8). Our preferred model fits are shown in Figure 4, while the model predicted slip rates and plate motions (relative to India) are shown in Figure 5. This model is one of the statistically acceptable representations of this tectonic region (minima in ABIC in Figure 7a) but does not reveal all the complexities or trade-offs in the information we have learned from studying the data. We elaborate on the robust results we have gathered from a suite of models below.

The observed convergence can be explained by assuming full coupling on the shallow section of the Rakhine-Bangladesh megathrust; the estimated slip rate on the megathrust varies spatially from 12 to 24 mm/year with an average of ~18 mm/year (Figure 7). The velocity field resulting from elastic dislocations is almost entirely east-west in the outer IBW (Figure 6d). Since we approximate the megathrust as a north-south structure, we obtain minimal strike-slip components; however, this would change if we make the megathrust more arcuate (Figure S8). We observe a significant difference in the geometry of the megathrust inferred from 2-D and 3-D models (Figures 6c and 6d). Two-dimensional models require an exaggerated arcuate shape for the megathrust, with the horizontal position of the coupling transition very close to the CMF; however, the misfit from such a model is significantly large compared to the block models in which we explicitly solved for fault geometry (Figure 6c), such that it can be ruled out at the 95% confidence level using an *F* test. Block models with different modeling choices, such as different penalties on the CMF or allowing

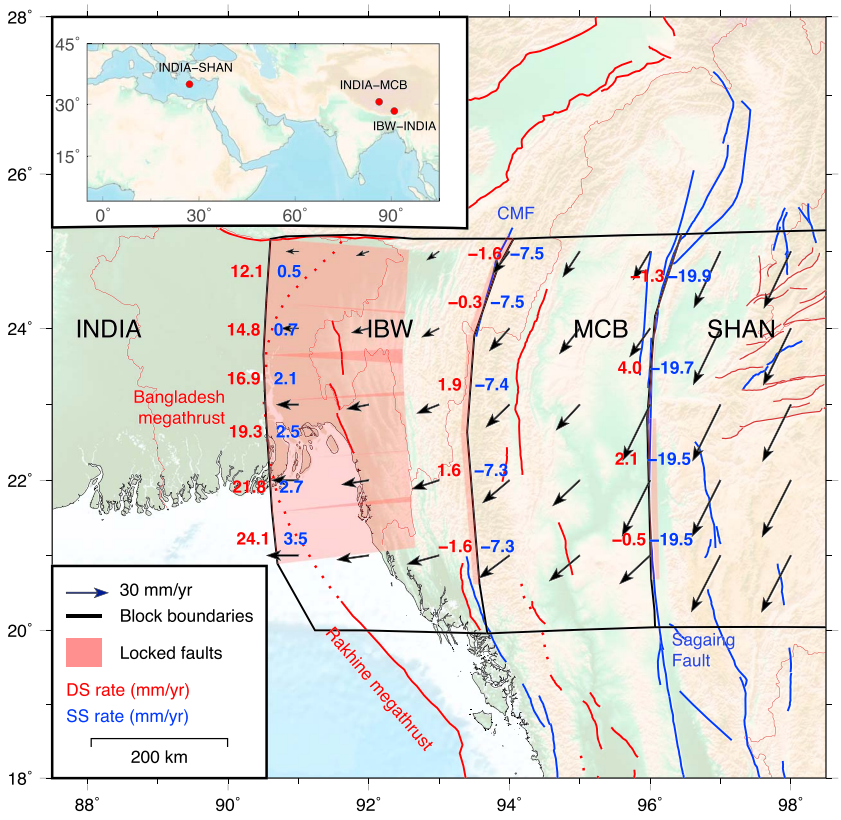

Figure 5. Results of the block modeling exercise; we show the results from our preferred model (Figure 4). The arrows show estimated plate motion vectors within the blocks relative to India in a regular grid. The inset figure shows the Euler poles computed for each of the blocks relative to India. The formal uncertainties from the model covariance matrix is approximately 0.2 mm/year for dip-slip and strike-slip rates on the fully coupled faults; however, a more realistic measure of uncertainty is ~2 mm/year and can be visualized from the range of mean slip rates in Figures S6–S8.
CMF = Churachandpur-Mao Fault; IBW = Indo-Burman Wedge; MCB = Myanmar Central Basin block.

internal strain in the IBW, vary in the estimated dip and depth of the coupling transition but yield a robust estimate of the horizontal location of the coupling transition for the Rakhine-Bangladesh megathrust (Figures 6a, 6b, and 6d). We chose a preferred block model using ABIC: the model with $\sigma_{CMF} = 4$ mm/year and no internal strain in the IBW (Figures 7a and S10).

The slip rate estimates of the CMF are not very robust and trade off significantly with possible internal deformation within the IBW (Figures 6d and 7). However, we observe that in all our models there needs to be a northward translation of the inner IBW even though the mechanism is unclear. Models in which we permit internal strain rate within the IBW almost entirely shut off the CMF while producing a velocity field remarkably similar to that expected for a purely right-lateral strike-slip fault (Figures 6d and 7). The ABIC values of these models are greater than that of the preferred model, but they cannot be rejected at the 95% confidence level of an *F* test (Figure S10). This means that even though we cannot be certain of the mechanism of deformation in the inner IBW, there must be dextral slipping fault(s) that accommodate this deformation. In models in which we do not impose any constraints on the rake of the CMF, the model adds some thrust and normal motion along segments of the fault, which appears to be unphysical (Figures 7, S7, and S8). A more careful study of the variation of the inferred rake when varying the strength of the dip-slip penalization on the CMF also shows that the rake becomes more variable and tends to predict significant dip-slip when the penalization is weak (Figure 7). This is an artifact of fitting noisy data that we do not think is geologically relevant, and thus we use the requirement of limited fault-perpendicular motion on the CMF to place an upper bound on its possible strike-slip rate at ~8 mm/year (Figure 7).

The slip rate on the Sagaing Fault (~19.5 mm/year) falls within our prior assumption of 20 ± 2 mm/year dextral strike slip. We apply these priors because the slip rate on the Sagaing Fault can be independently

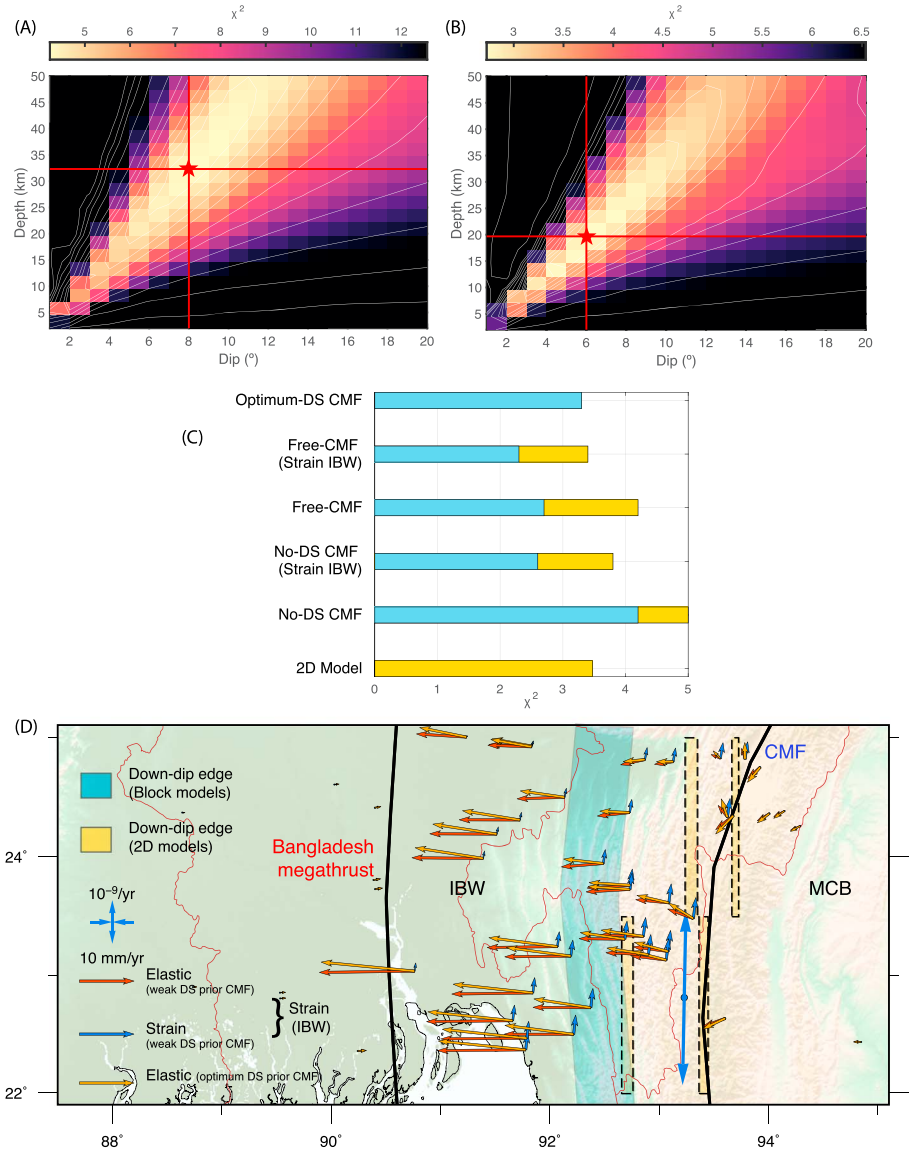

Figure 6. (a and b) Results of grid search for dip and depth of the Rakhine-Bangladesh megathrust using 3-D rigid block models. We apply a dip-slip prior of 0 ± 1 mm/year on the CMF (a) and no priors on the CMF in (b). The red star indicates the best fitting (lowest misfit) model parameter. The contours show that the model is not very sensitive to dip (δ) and depth (d) independently, but is sensitive to $x_d = \frac{\delta}{\tan(D)}$ which is the horizontal location of the coupling transition, just like in the 2-D models (Text S1). (c) We compare the reduced χ^2 statistics of our different modeling choices. The golden yellow bars represented 2-D and 3-D block models whose geometries are constructed using the geometries inferred from the 2-D models, while the blue bars represent 3-D models in which we explicitly solved for the geometry of the Rakhine-Bangladesh megathrust. The misfits are significantly lower for the models inferred from 3-D block models. (d) The golden yellow regions show the 95% confidence interval of the horizontal position of the down-dip coupling transition inferred from 2-D models; the blue regions show the 95% confidence interval for the horizontal position of the coupling transition for the Rakhine-Bangladesh megathrust, inferred from all our 3-D block models. The red and blue arrows represent the velocities resulting from elastic deformation and the estimated strain rate tensor in the IBW, respectively (for a model with uniform strain rate within the IBW and a dip-slip prior on the CMF of 0 ± 10 mm/year). The strain rate tensor which shows ~N-S extension is shown in blue within the inner IBW. The orange arrows represent the velocities resulting from elastic dislocations for a model with elastic blocks and an optimized weight of the dip-slip prior on the CMF of 0 ± 4 mm/year. The velocities from elastic dislocations for the elastic block model are the resultant of the elastic and strain rate-derived velocities in the model with internal deformation in the IBW; this shows the trade-off between slip on the CMF and strain rates within the IBW. CMF = Churachandpur-Mao Fault; IBW = Indo-Burman Wedge; MCB = Myanmar Central Basin; DS prior = dip-slip prior (σ_{CMF} in Figure 7).

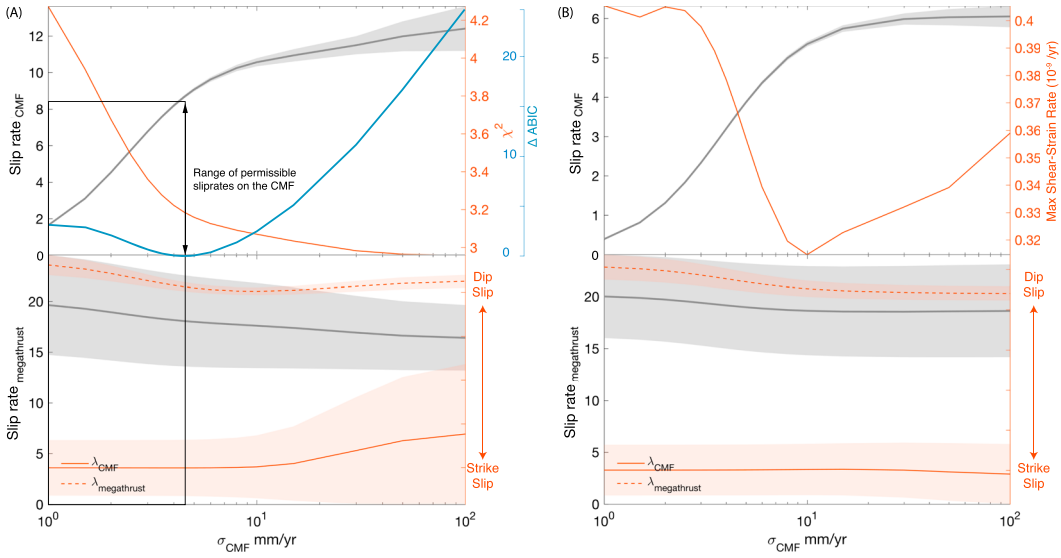

Figure 7. Trade-off curves for a priori constraints on the CMF. (a) Misfit statistics (ABIC in blue, and reduced χ^2 in orange) and fault parameters vary with the standard deviation σ_{CMF} of the prior dip-slip constraint on the CMF for rigid block models. At values of σ_{CMF}> 4 mm/year the inversion becomes unstable, as seen in the increased variability in λ_{CMF}(rake) and departure from strike-slip behavior. This gives us a range of permissible values of slip rate, 0–8 mm/year, for the CMF. (b) Model parameters show lesser variation with σ_{CMF} for block models where the Indo-Burman Wedge is allowed to deform internally compared to (a). Even as σ_{CMF} is increased to 100 mm/year, the slip rate on the CMF does not exceed 6 mm/year. ABIC = Akaike's Bayesian information criterion; CMF = Churachandpur-Mao Fault.

constrained in the two-dimensional models (Figure S5), and they improve the stability of the solution to our inverse problem. However, our model predicts a component of dip-slip motion on the Sagaing Fault as well, reaching ~4 mm/year at 24°N. To test if this observation is robust, we ran an experiment with an extra block in the northern Shan plateau, similar to the geometry of Socquet et al. (2006; Figure S8b). The addition of this block does not significantly affect the fit to the data but removes all dip-slip motion from the Sagaing Fault. Thus, we suggest that this dip-slip motion is a consequence of the lack of data to constrain the rotation rate of the northern Shan block. Since the stations in this block are close to faults in the Shan Plateau, these sites cannot independently capture the far-field velocity of the Sagaing Fault, requiring ad-hoc methods to account for the resulting distortion of the velocity field (Text S2.2; Maurin et al., 2010).

4. Discussion

In our modeling of the India-Burma-Sunda collision zone, we build complexity step by step: we start with two-dimensional models to find regions with large surface velocity gradients that likely correspond to coupling transitions on faults and then use those results to construct a kinematically consistent block model that can fit the velocities. From these models, we show that there is a significant component of convergence between the India and Burma plates that is not being released as creep, and that the data are most consistent with a large locked zone on the Rakhine-Bangladesh megathrust. This locked area (shown in red in Figures 4 and 5) most likely releases the accumulated strain intermittently through earthquakes, as observed for other locked faults worldwide. Given that this fault has been nearly seismically silent during the instrumental period we suggest that earthquakes on the megathrust and/or associated anticlinal structures may have a large (>500 years) recurrence interval, and that as a result these events may be large.

4.1. Geodetically Observable Convergence Across the Bangladesh Megathrust

Previous kinematic studies that used two-dimensional dislocations report contrasting results regarding convergence across the IBW, that is, from no convergence (Gahalaut et al., 2013) to 13–17 mm/year convergence (Steckler et al., 2016). Our 3-D block models of the India-Burma-Sunda system shows that a significant convergence rate across the Rakhine-Bangladesh megathrust is necessary to explain the India-Burma-Sunda plate motion vectors. The dip-slip component of the convergence across the Bangladesh megathrust decreases northward from 24 to 12 mm/year from 22°N to 25°N (Figures 5 and S6–S8) due to rotation of

the IBW relative to India. While the total convergence rate is well constrained, we cannot be certain which faults will ultimately accommodate this strain. The megathrust in our models represents a basal décollement underlying the Chittagong fold-and-thrust belt (Betka et al., 2018), and if it were to rupture as a single event it would represent a large, Cascadia-type earthquake. However, there are also a series of thrust faults and anticlines within this belt with unknown levels of seismic activity, though the geodetic data presented here largely rule out the possibility of significant aseismic convergence on these structures, as this would represent sources of strain occurring closer to the fault trace than supported by our modeling. Thus, seismic events on out-of-sequence thrusts are also a possibility, as occurred in the 1999 M_w 7.6 Chi-Chi earthquake in Taiwan (Yue et al., 2005), and the 2008 M_w 7.9 Wenchuan earthquake in China (Hubbard et al., 2010).

4.2. Strain Partitioning in the Burma Plate

Our models cannot uniquely constrain the slip rate of the CMF due to the strong trade-offs between models that permit dip-slip on the CMF versus models that penalize dip-slip on the CMF but allow internal deformation of the IBW. In Figures 6c and S10, we show the models which are hard to distinguish statistically (using ABIC and F tests); they allow anywhere between 0 and 13 mm/year of motion on the CMF (Figures S7 and S8). The most common interpretation of the geodetic data has been that the CMF is an active plate/sliver boundary fault (Gahalaut et al., 2013; Steckler et al., 2016), but in our models we show that this is not a robust result. We therefore ask the following: How do we know the CMF is active? Gahalaut et al. (2013) argue that there is surface creep observed in the GPS velocity field, and Wang et al. (2014) note that three to six river channels may be deflected by the CMF. However, our models demonstrate that there is no strong geodetic evidence for interseismic shallow creep in the current data, and that the velocity field can still be fit by a CMF that is fully coupled to a depth greater than 25 km (for a synthetic experiment to demonstrate the nonuniqueness of inferred shallow creep we refer the reader to Text S3 and Figure S3). Shallow creep along the entire fault is not necessary, and even unlikely, in a block model that considers the arcuate shape of the CMF and the megathrust (Figure 4 and S3). We do note that the survey-mode GPS stations HENG and CCPR (Figure 4b), which are merely 4 km apart, show significantly different north-south velocities that are not well fit in models with a fault that is coupled to a depth greater than 25 km. This indicates that either there is very local shallow creep near these stations, or that one or both stations have unexplained site effects that are affecting the geodetic signal. Continuous shallow interseismic creep has been observed on strike-slip faults (for a review see Harris (2017)), but we caution against interpreting widespread creep based on observations at just one location, and particularly against then using this to interpret activity of a major, block-bounding fault. Other evidence for an active CMF is also limited: the river channel deflections observed by Wang et al. (2014) are few and display offsets which are less than 3 km; they could instead represent a river flowing around preexisting topography, which follows bedding. Thus, invoking that the CMF is an active sliver boundary is difficult to defend. However, since our results indicate that there has to be some mechanism of northward transport (relative to India) in the inner IBW (Figures 6d, S7, and S8), we can state that the convergence is accommodated by the outer IBW while the inner IBW could be a shear zone that deforms in a north-south manner (Figure 8).

The IBW is juxtaposed against the MCB along the Kabaw Fault, which has been hypothesized to accommodate ~6 mm/year of oblique slip (Steckler et al., 2016). However, we find no need to invoke slip on this fault to fit our data in either our two-dimensional or block models. The MIBB network adds two new continuous GPS stations HAKA and KANI (Figure 4) on either side of the fault which show <3 mm/year difference in their velocities relative to India. This small difference can be fully reconciled as a combination of the Burma plate rotation and the effect of strain accumulation on the down-dip extension of the Rakhine-Bangladesh megathrust and/or CMF. The data do not require that the Kabaw Fault be inactive, but its slip rate must be within the modeling uncertainties, likely <2–3 mm/year. Geologic observations along the Kabaw Fault corroborate this inference and suggest that its slip rate is less than the sedimentation rate, so that if there is any young deformation, it is buried (Wang et al., 2014).

Along the eastern edge of the Burma plate, the Sagaing Fault takes up ~20 mm/year of dextral strike slip. This is consistent with previous geodetic studies of the northern and central transects (Maurin et al., 2010; Vigny et al., 2003) as well as Quaternary slip rate estimates of the Sagaing Fault (Bertrand et al., 1998). The total shearing rate between India and the Shan Block, accommodated by fully coupled faults is ~30 mm/year, lower than previously inferred rates of up to ~40 mm/year (Gahalaut et al., 2013; Steckler

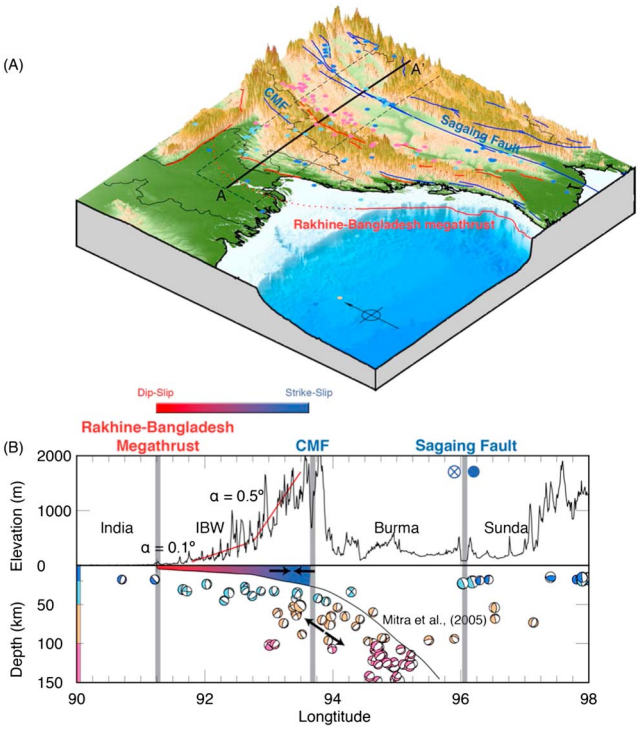

Figure 8. (a) Perspective view of the study area with faults and earthquake epicenters from GCMT superimposed on top. AA′ shows the location of the swath profile considered in (b). (b) Topographic profile and depth profile for a 100-km swath along AA′. The outer wedge is one of the flattest in the world with $\alpha \sim 0.1°$ (topographic slope); the inner wedge is steeper with $\alpha \sim 0.5°$. This transition also happens to be the point where we infer a coupling transition in our models. The plate interface, shown as the thin black line in the depth profile, is taken from Mitra et al. (2005). We hypothesize that Indo-Burma plate motion is accommodated on the megathrust, CMF, and/or other unmapped structures in the IBW. The red to blue color transition in the IBW depth profile represents the likelihood of dip-slip (red) to strike-slip (blue) motion on faults within the IBW (see section 4.2 for the explanation). We also show GCMT earthquake focal mechanisms, colored by depth, in cross-sectional view along AA′. The extensional axes of the intraslab earthquakes follow the slab dip, while the upper plate appears to be in arc-normal compression. This suggests that subduction is active.
CMF = Churachandpur Mao Fault; IBW = Indo-Burman Wedge; GCMT = Global Centroid Moment Tensor.

et al., 2016), since these previous studies neglected block rotations (Text S2; compare Figures S2c and Figures S6 and S7).

From our models, we infer that the Rakhine-Bangladesh megathrust and the Sagaing Fault act as block-bounding faults for the Burma plate, while the CMF may be a backstop to the IBW or a nascent block boundary (Figure 8). If the CMF is a major strike-slip fault partitioning some of the oblique convergence between India and Burma plates, then the slip rate cannot exceed an average of 8 mm/year along its entire length (Figure 7). We posit end-member models of this tectonic environment as follows:

1. E-W compressional strain is being accumulated within the outer wedge, most likely associated with the Rakhine-Bangladesh megathrust while N-S shearing is accommodated within the inner wedge. This shear may have localized onto a single fault, the CMF, and the upper bound of its slip rate is 8 mm/year (Figures S7c and S7d).
2. The IBW and MCB are a single rotating block relative to India, thereby defining the Burma plate (Figures S6a–S6c). The IBW is the internally deforming portion of the Burma plate, while the MCB is rigid. The Rakhine-Bangladesh megathrust accommodates convergence between India and Burma while the obliquity in plate motion has not localized onto the CMF but is instead distributed within the inner IBW (Figure 8).

With a first-order understanding of the tectonics of the India-Burma-Sunda plate system (Figure 8), we comment on the subduction of the Indian slab beneath Burma as well as the earthquake likelihood of the Rakhine-Bangladesh megathrust.

4.3. Continued Subduction of the Indian Slab

Our ensemble of block models suggests that there is significant active interblock convergence across the Rakhine-Bangladesh megathrust (Figures 5 and S6–S8), but we are unable to describe the forces that cause this convergence since block modeling is only a kinematic description of the observations. However, we can test the validity of some first-order geodynamic hypotheses based on combined insight from geodetic, geological, and seismological observations.

Some authors have suggested that the subduction of the Indian slab beneath Burma has ceased in the Quaternary (or for even longer) and propose that gravitational collapse of the Tibetan plateau drives the observed shortening of the IBW (e.g., Rangin et al., 2013). The hypothesis is that the observed slab parallel tensional axes in the Indian slab indicate ceased subduction, while the observed foldbelt-perpendicular compressional axes in the IBW are assumed to be a consequence of topographically driven flow of material from the Tibetan plateau into the MCB and thus shortening the IBW, or the IBW itself is over-steepened and is collapsing. The aforementioned interpretation of earthquake data is likely flawed, since slab parallel tensional axes are linked to cold, negatively buoyant slabs that have not yet reached the 660-km discontinuity (Isacks & Molnar, 1971) and the aforementioned stress axes orientations in the slab as well as upper plate (Figure 8b) have been observed in many active subduction zones, such as in the Andaman, Kyushu, and Cascadia subduction zones (Mallick et al., 2017; Seno & Yoshida, 2004).

The stresses from gravity driven tectonics are normally manifested as a series of strike-slip or normal faults in the back of the fold-and-thrust belt (e.g., as seen in the Niger delta; Corredor et al., 2005). However, we have two results from our study that challenge this notion. (1) We can fit the velocities in the MCB using the rigid elastic block assumption implying that the velocities arising from gravitational potential energy collapse of either the Shan Plateau or the IBW do not extend to the MCB. (2) We do not observe normal

faulting or extension within the inner IBW; even in models in which we allow internal deformation of the IBW, the sense of motion is north-south shear (strain rate tensor in Figure 6d) implying that gravity tectonics is an unlikely explanation for the observed convergence in the outer IBW.

Thus, even though we cannot explicitly discriminate between the forces driving the active India-Burma convergence, the geodetic, seismological and geologic evidence can be explained by an active subduction zone.

4.4. Earthquake Hazard Due to the Rakhine-Bangladesh Megathrust

The IBW hosts one of the world's flattest accretionary prisms, with ~0.1° slope for the outer wedge, and has a very shallow décollement (Betka et al., 2018; Burgi et al., 2016). This implies that the detachment is very weak, possibly in part because fluid overpressures on the décollement seem to be nearly lithostatic (Steckler et al., 2008; Zahid & Uddin, 2005). These observations, together with the lack of interplate seismicity in the instrumental catalog, have been used to suggest that the Rakhine-Bangladesh megathrust creeps continuously or periodically to relieve strain (Kundu & Gahalaut, 2012; le Dain et al., 1984; Ni et al., 1989). We note that a lack of microseismicity is not diagnostic of ceased fault activity; the Cascadia subduction zone is a good example of an active megathrust in a high sedimentation setting which exhibits very few moderate-sized earthquakes in the modern catalog, but which is known to produce occasional M~9 events (Nelson et al., 1995). Here we demonstrate that the geodetic data in Bangladesh (Figures 2 and S2) do not show any evidence of creep, which would manifest as a sharp offset in velocity at the fault trace. Instead, there is a signal of interplate coupling and strain accumulation (Figure 4).

The lack of surface fault creep is not in conflict with observations of fluid overpressure and low friction at shallow depths (Steckler et al., 2008; Zahid & Uddin, 2005). The absence of creep is an observation of strong interplate coupling, but it does not imply that the shallow megathrust is frictionally locked (we refer the reader to Table 1 in Almeida et al., 2018, for definitions). A down-dip locked zone is expected to create stress shadows on the shallow megathrust that will limit the creep rate to a small fraction of the plate rate, irrespective of the frictional properties (Almeida et al., 2018). This results in accumulation of a slip deficit during the interseismic period, even on fault patches that are frictionally unlocked or unclamped.

The most recent great earthquake along the Rakhine megathrust is the M~8 1762 Great Arakan Earthquake (Halsted, 1841); the average recurrence interval of major plate boundary rupturing events in this area may be 500–1000 years (Aung et al., 2008; Wang et al., 2013). This suggests that even if the shallow megathrust is frictionally unlocked, there may be locked patches at greater depths that can nucleate earthquakes that propagate into the shallow part of the fault. Such earthquakes may produce sudden coastal uplift and resulting tsunamis (Cummins, 2007) and be recorded by corals and terraces (Wang et al., 2013). We can draw similar inferences about possible earthquakes on the subaerial Bangladesh megathrust, but we have minimal information about earthquakes on this fault. To date, the Great Bengal earthquake of 1548 is the only M~8+ event hypothesized to have ruptured the Bangladesh megathrust, although it alternatively or in addition may have been caused by slip on the Dauki Thrust (Morino et al., 2011; Steckler et al., 2008).

Our models suggest that the megathrust is fully coupled all the way from the deformation front to an arcuate line beneath the high IBR (Figure 6d). The maximum strain accumulation on the Rakhine-Bangladesh megathrust is 20 ± 5 mm/year, for models with high dip-slip penalization on the CMF (Figure 7a). This could be used as a limiting scenario for seismic hazard models for this area. The most likely estimate, supported by objective model selection, is 18 ± 4 mm/year (Figures 7a and S10). The continuous GPS time series do not show any obvious time-varying creep/slow-slip episodes during the period 2011–2017 (Figures 3 and S9). We rule out the possibility that the megathrust is creeping interseismically, although some limited patches within the megathrust could potentially host creep phenomena (time-invariant or time-varying) that are within the measurement uncertainties. Thus, there is almost certainly ongoing strain accumulation on the megathrust, which will eventually be released either in an earthquake or as postseismic creep following earthquakes on more limited patches.

5. Conclusions

The IBR are part of a fold-and-thrust belt that formed as a result of oblique India-Sunda plate collision. This collision manifests as a complex system of slip partitioning between multiple faults spread over the Burma plate. We use a new continuous GPS data set from the MIBB network to model the horizontal deformation

field over an area spanning ~1000 km from Bangladesh to Myanmar. We use elastic dislocations, horizontal strain rates, and block-like motion on a sphere to model the horizontal velocities obtained from our stations, together with published data sets, and find the following:

1. We infer active convergence across the IBR at a rate of ~12–24 mm/year. The India and Burma plates are fully coupled to a depth of ~30 km, and the surface projection of the deep coupling transition follows the trend of the high IBR, ~200 km east of the modern deformation front.
2. We estimate dextral shear of ~8 mm/year across the IBW, distributed between the CMF and/or other unresolved upper plate structures. The Sagaing Fault takes up ~20 mm/year of dextral shear, resulting in a total north-south shear of ~30 mm/year between India and Sunda.
3. We fit the horizontal velocity field well using a block model with fully coupled faults and show that simplified modeling in two dimensions can cause significant biases in the results, such as implying creep on the CMF or large slip rates on the Kabaw Fault.
4. Based on geological observations, we suggest that, to a first order, the deep India-Burma plate interface accommodates ~12–24 mm/year of oblique India-Burma motion, which may further be partitioned among various upper plate structures in the seismic cycle.
5. The absence of notable interplate seismicity on the shallow part of the megathrust during the past 100 years does not imply that the megathrust cannot nucleate large earthquakes.

Acknowledgments
This research is supported by the National Research Foundation of Singapore and the Singapore Ministry of Education under the Research Centres of Excellence initiative and its Singapore NRF Fellowship scheme (National Research Fellow awards NRFF2010-64 and NRFF2013-06). All the figures in this paper were made using GMT (Wessel & Smith, 1998) and MATLAB. This work comprises Earth Observatory of Singapore contribution 235. The authors thank Kyle Bradley, Wang Yu, Roland Bürgmann, Paul Tapponnier, and Kerry Sieh for useful discussions; the staff at the Technical Office (EOS) and our collaborators at the Department of Meteorology and Hydrology, Myanmar (Kyaw Moe Oo), Myanmar Earthquake Committee (U. Nyut Maung San), North Eastern Hill University (Devesh Walia), Geological Survey of Bangladesh (Aktarul Ahsan), and Sherubtse College, Royal University of Bhutan (Bimal Sharma) for helping install and maintain the MIBB network; and Pavel Adamek for linguistic advice. We thank two anonymous reviewers and the Editor at JGR for comments and feedback that helped improve this manuscript. All GPS velocities (from this study and previously published studies) used in our plate motion models are presented in supporting information Table S1. The GPS rinex files used in this study are available at the website (ftp://datacollection.earthobservatory.sg/MIBB_cGPS_2011-2017).

References

Almeida, R., Lindsey, E. O., Bradley, K., Hubbard, J., Mallick, R., & Hill, E. M. (2018). Can the updip limit of frictional locking on megathrusts be detected geodetically? Quantifying the effect of stress shadows on near-trench coupling. *Geophysical Research Letters*, *45*, 4754–4763. https://doi.org/10.1029/2018GL077785

Altamimi, Z., Collilieux, X., & Métivier, L. (2011). ITRF2008: An improved solution of the international terrestrial reference frame. *Journal of Geodesy*, *85*(8), 457–473. https://doi.org/10.1007/s00190-011-0444-4

Altamimi, Z., Métivier, L., & Collilieux, X. (2012). ITRF2008 plate motion model. *Journal of Geophysical Research*, *117*, B07402. https://doi.org/10.1029/2011JB008930

Aung, T. T., Satake, K., Okamura, Y., Shishikura, M., Swe, W., Saw, H., et al. (2008). Geologic evidence for three great earthquakes in the past 3400 years off Myanmar. *Journal of Earthquake and Tsunami*, *02*(04), 259–265. https://doi.org/10.1142/S1793431108000335

Bertrand, G., Rangin, C., Maury, R. C., Htun, H. M., Bellon, H., & Guillaud, J. P. (1998). Les basaltes de Singu (Myanmar): Nouvelles contraintes sur le taux de décrochement récent de la faille de Sagaing. *Comptes Rendus de l'Académie des Sciences - Series IIA - Earth and Planetary Science*, *327*(7), 479–484. https://doi.org/10.1016/S1251-8050(99)80076-7

Betka, P. M., Seeber, L., Thomson, S. N., Steckler, M. S., Sincavage, R., & Zoramthara, C. (2018). Slip-partitioning above a shallow , weak décollement beneath the Indo-Burman accretionary prism. *Earth and Planetary Science Letters*, *503*, 17–28. https://doi.org/10.1016/j.epsl.2018.09.003. https://doi.org/10.1029/98JB02467

Bijwaard, H., Spakman, W., & Engdahl, E. R. (1998). Closing the gap between regional and global travel time tomography. *Journal of Geophysical Research*, *103*(B12), 30,055–30,078. https://doi.org/10.1029/98JB02467

Bradley, K. E., Feng, L., Hill, E. M., Natawidjaja, D. H., & Sieh, K. (2017). Implications of the diffuse deformation of the Indian Ocean lithosphere for slip partitioning of oblique plate convergence in Sumatra. *Journal of Geophysical Research: Solid Earth*, *122*, 572–591. https://doi.org/10.1002/2016JB013549

Brunnschweiler, R. O. (1966). On the geology of the Indoburman ranges. *Journal of the Geological Society of Australia*, *13*(1), 137–194. https://doi.org/10.1080/00167616608728608

Burgi, P., Hubbard, J., Peterson, D. E., & Akhter, S. H. (2016). Fault geometry beneath the Chittagong-Myanmar fold and thrust belt, Bangladesh, and implications for earthquake hazard. In American Geophysical Union, Fall General Assembly 2016, Abstract id. T13D-03. https://doi.org/2016AGUFM.T13D..03B

Corredor, F., Shaw, J. H., & Bilotti, F. (2005). Structural styles in the deep-water fold and thrust belts of the Niger Delta. *AAPG Bulletin*, *89*(6), 753–780. https://doi.org/10.1306/02170504074

Cummins, P. R. (2007). The potential for giant tsunamigenic earthquakes in the northern Bay of Bengal. *Nature*, *449*(7158), 75–78. https://doi.org/10.1038/nature06088

le Dain, A. Y., Tapponnier, P., & Molnar, P. (1984). Active faulting and tectonics of Burma and surrounding regions. *Journal of Geophysical Research*, *89*(B1), 453. https://doi.org/10.1029/JB089iB01p00453

Feng, L., Hill, E. M., Banerjee, P., Hermawan, I., Tsang, L. L. H., Natawidjaja, D. H., et al. (2015). A unified GPS-based earthquake catalog for the Sumatran plate boundary between 2002 and 2013. *Journal of Geophysical Research: Solid Earth*, *120*, 3566–3598. https://doi.org/10.1002/2014JB011661

Funning, G. J., Fukahata, Y., Yagi, Y., & Parsons, B. (2014). A method for the joint inversion of geodetic and seismic waveform data using ABIC: Application to the 1997 Manyi, Tibet, earthquake. *Geophysical Journal International*, *196*(3), 1564–1579. https://doi.org/10.1093/gji/ggt406

Gahalaut, V. K., Kundu, B., Laishram, S. S., Catherine, J., Kumar, A., Singh, M. D., et al. (2013). Aseismic plate boundary in the Indo-Burmese wedge, northwest Sunda Arc. *Geology*, *41*(2), 235–238. https://doi.org/10.1130/G33771.1

Halsted, E. . (1841). Report on the Island of Chedooba. Journal of the Asiatic Society of Bengal.

Harris, R. A. (2017). Large earthquakes and creeping faults. *Reviews of Geophysics*, *55*, 169–198. https://doi.org/10.1002/2016RG000539

Herring, T. (2003). MATLAB tools for viewing GPS velocities and time series. *GPS Solutions*, *7*(3), 194–199. https://doi.org/10.1007/s10291-003-0068-0

Hubbard, J., Shaw, J. H., & Klinger, Y. (2010). Structural setting of the 2008 Mw 7.9 Wenchuan, China, earthquake. *Bulletin of the Seismological Society of America*, *100*(5 B), 2713–2735.

Isacks, B., & Molnar, P. (1971). Distribution of stresses in the descending lithosphere from a global survey of focal mechanisms solutions of mantle earthquake. *Reviews of Geophysics and Space Physics*, *9*(1), 175–193.
Kreemer, C., Blewitt, G., & Klein, E. C. (2014). A geodetic plate motion and Global Strain Rate Model. *Geochemistry, Geophysics, Geosystems*, *15*, 3849–3889. https://doi.org/10.1002/2014GC005407
Kundu, B., & Gahalaut, V. K. (2012). Earthquake occurrence processes in the Indo-Burmese wedge and Sagaing fault region. *Tectonophysics*, *524-525*, 135–146. https://doi.org/10.1016/j.tecto.2011.12.031
Lindsey, E. O., & Fialko, Y. (2013). Geodetic slip rates in the southern San Andreas fault system: Effects of elastic heterogeneity and fault geometry. *Journal of Geophysical Research: Solid Earth*, *118*, 689–697. https://doi.org/10.1029/2012JB009358
Mallick, R., Parameswaran, R. M., & Rajendran, K. (2017). The 2005 and 2010 earthquakes on the Sumatra–Andaman trench: Evidence for post-2004 megathrust intraplate rejuvenation. *Bulletin of the Seismological Society of America*, *107*(3). https://doi.org/10.1785/0120160147
Mansinha, L., Smyli, E., & D. (1971). The displacement field of inclined faults. *Bulletin of the Seismological Society of America*, *61*(5), 1433–1440.
Maurin, T., Masson, F., Rangin, C., Min, U. T., & Collard, P. (2010). First global positioning system results in northern Myanmar: Constant and localized slip rate along the Sagaing fault. *Geology*, *38*(7), 591–594. https://doi.org/10.1130/G30872.1
Maurin, T., & Rangin, C. (2009). Structure and kinematics of the Indo-Burmese wedge: Recent and fast growth of the outer wedge. *Tectonics*, *28*, TC2010. https://doi.org/10.1029/2008TC002276
McCaffrey, R. (2002). Crustal block rotations and plate coupling. In S. Stein & J. Freymueller (Eds.), *Plate Boundary Zones, AGU Geodynamics Series 30* (pp. 101–122). Washington, DC: American Geophysical Union. https://doi.org/10.1029/GD030p0101
Meade, B. J., & Loveless, J. P. (2009). Block modeling with connected fault-network geometries and a linear elastic coupling estimator in spherical coordinates. *Bulletin of the Seismological Society of America*, *99*(6), 3124–3139. https://doi.org/10.1785/0120090088. https://doi.org/10.1785/0120090088
Meng, J., Wang, C., Zhao, X., Coe, R., Li, Y., & Finn, D. (2012). India-Asia collision was at 24°N and 50 Ma: Palaeomagnetic proof from southernmost Asia. *Scientific Reports*, *2*(1), 925. https://doi.org/10.1038/srep00925
Menke, W. (2012). *Discrete inverse theory. Geophysical data analysis: Discrete inverse theory*. Oxford, UK: Geophysical Data Analysis. https://doi.org/10.1016/C2011-0-69765-0
Morino, M., Maksud Kamal, A. S. M., Muslim, D., Ekram Ali, R. M., Kamal, M. A., Zillur Rahman, M., & Kaneko, F. (2011). Seismic event of the Dauki fault in 16th century confirmed by trench investigation at Gabrakhari Village, Haluaghat, Mymensingh, Bangladesh. *Journal of Asian Earth Sciences*, *42*(3), 492–498. https://doi.org/10.1016/j.jseaes.2011.05.002
Neal, R. M. (2003). Slice sampling. *The Annals of Statistics*, *31*(3), 705–767. https://doi.org/10.1214/aos/1056562461
Nelson, A. R., Atwater, B. F., Bobrowsky, P. T., Bradley, L. A., Clague, J. J., Carver, G. A., et al. (1995). Radiocarbon evidence for extensive plate-boundary rupture about 300 years ago at the Cascadia subduction zone. *Nature*, *378*(6555), 371–374. https://doi.org/10.1038/378371a0
Ni, J. F., Guzman-Speziale, M., Bevis, M., Holt, W. E., Wallace, T. C., & Seager, W. R. (1989). Accretionary tectonics of Burma and the three-dimensional geometry of the Burma subduction zone. *Geology*, *17*(1), 68–71. https://doi.org/10.1130/0091-7613(1989)017<0068:ATOBAT>2.3.CO;2
Nielsen, C., Chamot-Rooke, N., & Rangin, C. (2004). From partial to full strain partitioning along the Indo-Burmese hyper-oblique subduction. *Marine Geology*, *209*(1–4), 303–327. https://doi.org/10.1016/j.margeo.2004.05.001
Okada, Y. (1986). Surface deformation due to shear and tensile faults in a half-space. *Bulletin of the Seismological Society of America*, *23*(4), 128–1154. https://doi.org/10.1016/0148-9062(86)90674-1
Pesicek, J. D., Thurber, C. H., Zhang, H., Deshon, H. R., Engdahl, E. R., & Widiyantoro, S. (2010). Teleseismic double-difference relocation of earthquakes along the Sumatra-Andaman subduction zone using a 3-D model. *Journal of Geophysical Research*, *115*, B10303. https://doi.org/10.1029/2010JB007443
Radhakrishna, M., Subrahmanyam, C., & Damodharan, T. (2010). Thin oceanic crust below Bay of Bengal inferred from 3-D gravity interpretation. *Tectonophysics*, *493*(1–2), 93–105. https://doi.org/10.1016/j.tecto.2010.07.004
Rangin, C., Maurin, T., & Masson, F. (2013). Combined effects of Eurasia/Sunda oblique convergence and east-Tibetan crustal flow on the active tectonics of Burma. *Journal of Asian Earth Sciences*, *76*, 185–194. https://doi.org/10.1016/j.jseaes.2013.05.018
Rao, N. P., & Kalpna (2005). Deformation of the subducted Indian lithospheric slab in the Burmese arc. *Geophysical Research Letters*, *32*, L05301. https://doi.org/10.1029/2004GL022034
Raoof, J., Mukhopadhyay, S., Koulakov, I., & Kayal, J. R. (2017). 3-D seismic tomography of the lithosphere and its geodynamic implications beneath the northeast India region. *Tectonics*, *36*, 962–980. https://doi.org/10.1002/2016TC004375
Savage, J. C. (1983). A dislocation model of strain accumulation and release at a subduction zone. *Journal of Geophysical Research*, *88*, 4984–4996. https://doi.org/10.1029/JB088iB06p04984
Segall, P. (2010). *Earthquake and volcano deformation. Van Nostrand's scientific encyclopedia*. Princeton: Princeton University Press. https://doi.org/10.1515/9781400833856
Seno, T., & Yoshida, M. (2004). Where and why do large shallow intraslab earthquakes occur? *Physics of the Earth and Planetary Interiors*, *141*(3), 183–206. https://doi.org/10.1016/j.pepi.2003.11.002
Sloan, R. A., Elliott, J. R., Searle, M. P., & Morley, C. K. (2017). Chapter 2 Active tectonics of Myanmar and the Andaman Sea. *Geological Society, London, Memoirs*, *48*(1), 19–52. https://doi.org/10.1144/M48.2
Socquet, A., Vigny, C., Chamot-Rooke, N., Simons, W., Rangin, C., & Ambrosius, B. (2006). India and Sunda plates motion and deformation along their boundary in Myanmar determined by GPS. *Journal of Geophysical Research*, *111*, L19309. https://doi.org/10.1029/2005JB003877
Steckler, M. S., Akhter, S. H., & Seeber, L. (2008). Collision of the Ganges-Brahmaputra Delta with the Burma arc: Implications for earthquake hazard. *Earth and Planetary Science Letters*, *273*(3–4), 367–378. https://doi.org/10.1016/j.epsl.2008.07.009
Steckler, M. S., Mondal, D. R., Akhter, S. H., Seeber, L., Feng, L., Gale, J., et al. (2016). Locked and loading megathrust linked to active subduction beneath the Indo-Burman Ranges. *Nature Geoscience*, *9*(8), 615–618. https://doi.org/10.1038/ngeo2760. https://doi.org/10.1038/ngeo2760
Syracuse, E. M., van Keken, P. E., & Abers, G. A. (2010). The global range of subduction zone thermal models. *Physics of the Earth and Planetary Interiors*, *183*(1–2), 73–90. https://doi.org/10.1016/j.pepi.2010.02.004
Thatcher, W. (2007). Microplate model for the present-day deformation of Tibet. *Journal of Geophysical Research*, *112*, B01401. https://doi.org/10.1029/2005JB004244
Uddin, A., & Lundberg, N. (1998). Cenozoic history of the Himalayan-Bengal system: Sand composition in the Bengal basin, Bangladesh. *Bulletin of the Geological Society of America*, *110*(4), 497–511. https://doi.org/10.1130/0016-7606(1998)110<0497:CHOTHB>2.3.CO;2

Vigny, C., Socquet, A., Rangin, C., & Chamot-Rooke, N. (2003). Present-day crustal deformation around Sagaing fault, Myanmar. *Journal of Geophysical Research*, *108*(B11), 2533. https://doi.org/10.1029/2002JB001999

Wang, Y., Shyu, J. B. H., Sieh, K., Chiang, H. W., Wang, C. C., Aung, T., et al. (2013). Permanent upper plate deformation in western Myanmar during the great 1762 earthquake: Implications for neotectonic behavior of the northern Sunda megathrust. *Journal of Geophysical Research: Solid Earth*, *118*, 1277–1303. https://doi.org/10.1002/jgrb.50121

Wang, Y., Sieh, K., Tun, S. T., Lai, K.-Y., & Myint, T. (2014). Active tectonics and earthquake potential of the Myanmar region. *Journal of Geophysical Research: Solid Earth*, *119*, 3767–3822. https://doi.org/10.1002/2013JB010762

Wessel, P., & Smith, W. H. F. (1998). New, improved version of generic mapping tools released. *Eos, Transactions American Geophysical Union*, *79*(47), 579–579. https://doi.org/10.1029/98EO00426

Yue, L. F., Suppe, J., & Hung, J. H. (2005). Structural geology of a classic thrust belt earthquake: The 1999 Chi-Chi earthquake Taiwan (Mw= 7.6). *Journal of Structural Geology*, *27*(11), 2058–2083. https://doi.org/10.1016/j.pepi.2010.02.004

Zahid, K. M., & Uddin, A. (2005). Influence of overpressure on formation velocity evaluation of Neogene strata from the eastern Bengal Basin, Bangladesh. *Journal of Asian Earth Sciences*, *25*(3), 419–429. https://doi.org/10.1016/j.jseaes.2004.04.003